IEEE Access
Multidisciplinary ⋮ Rapid Review ⋮ Open Access Journal

Received 19 September 2023, accepted 8 October 2023, date of publication 10 October 2023, date of current version 17 October 2023.

Digital Object Identifier 10.1109/ACCESS.2023.3323583

RESEARCH ARTICLE

Communication Energy Analysis in Soft Robotic and Artificial Skin Covered Structures Using Modified X-Node WBAN Network

MAHMOUD Z. ISKANDARANI, (Member, IEEE)
Faculty of Engineering, Al-Ahliyya Amman University, Amman 19328, Jordan
e-mail: m.iskandarani@ammanu.edu.jo

ABSTRACT In this work, effect of using robotic materials on energy consumption is examined and modelled as a function of path loss coefficient affecting communication paths between sensor nodes. This is important, as the path loss coefficient for soft robotics materials or ones that are skin-covered is similar to the wearable garment by humans with sensors, forming a wireless body area networks (WBANs). The simulation and analysis results demonstrated that there is a power relationship between residual energy and both transmitted data packets and path loss coefficient, which connects energy to path loss. The research established a relationship between residual energy and data size, and a relationship between residual energy and path loss coefficient. The research also showed that a communication channel network will collapse if the planned and desired data to be transferred is greater than the device's rated data capacity. These discoveries are crucial because they help choose the optimum nodes count for data rate and optimize the number of nodes to reduce the rate of energy depletion. Additionally, it aids in estimating how long a device can operate before the need for recharge. The mathematical equations created as a consequence of simulation are highly helpful in selecting the number of nodes and path loss coefficient of the structural materials used in robotics. The work employed a modified X-shape node distribution to offer thorough robotic body coverage and a number of deviant pathways or routes. The work enables WBAN design optimization using robots, before using nodes distribution within WBAN on humans.

INDEX TERMS Energy, path loss, wearable sensors, data transmission, communication, WBAN, RWSN, soft robots, artificial skin.

I. INTRODUCTION

The sophistication of robots has grown tremendously, driven by applications in manufacturing automation. The shortcomings of conventional robots, such as safety while interacting with humans, resilience to disturbances, and adaptability to varied jobs and locations, became apparent during the progressive replacement of the assembly line by robots. Current research is focused on creating soft robotic bodies that can mimic the mobility and functions of biological ones. The objective is to create soft materials that has similar characteristics to biological tissues [1], [2].

Materials are developed to enable design of soft robotic structures, to be used in real-life applications. These materials include gels, soft elastomers, and soft polymer composites, among others [3], [4]. Often, a robot is an evolution of robotic technology, where robots are created primarily by drawing inspiration from biological living things and the natural world. The typical hard robot, is primarily made up of robust links and joints. In contrast, soft robots are constructed of elastic materials that are flexible and deformable [5], [6].

Robotic technology is now being developed employing rigid and semi-rigid materials. With soft and highly flexible material, robots can act and move in a manner close to bio-organisms. The use of soft and flexible materials is best approach to resolve a number of crucial issues in robotic

The associate editor coordinating the review of this manuscript and approving it for publication was Adamu Murtala Zungeru.

technology, despite the success of robotic systems made of stiff and semi-rigid materials [7], [8].

The robot can be covered with elastic materials like elastomers without affecting its mobility. For wearable supportive robotic systems, compatibility of this type of artificial skin is crucial. Additionally, the newly developed technologies are leveraging these flexible, intelligent, and soft materials [9].

Soft robots display qualities of infinite degrees of freedom (DOF) and nonlinear materials that need advances in control systems, making them fundamentally different from conventional rigid robots. The rapid advancement of materials design, robotics, and intelligent systems has resulted to a wide variety of novel control schemes being made possible by the diversification of actuator mechanisms, techniques, and algorithms [10], [11].

Emerging soft robots use conventional and soft sensors that operate as part of closed-loop feedback control. The stretchy body of the soft robot allows for programmable actuating behaviors and automated manipulations. This places high demands on the integrated sensors in terms of customized sensor characteristics, high-throughput data processing, and quick decision-making [12], [13], [14].

Robotic Wireless Sensor Networks (RWSN) is a general term combing robotic structures with communicating nodes. This covers Wireless Sensor Networks (WSNs) operating on robotic, but mainly, rigid structures [15], [16], [17], [18]. This enables separate energy computation and path loss calculation as the materials are rigid with specific properties, and Wireless Body area Networks (WBANs) operating on semi-rigid and soft robotic structures, including wearable robotics. This is due to the used soft materials, which makes energy consumption and path loss values close to human ones [19], [20].

If we consider the use-case of a soft robot, the robot must be able to communicate within itself and with its surroundings. Such communication should occur over a dedicated channel for compatibility in terms of frequency, data rate, voltages, and bandwidth. For Soft tissue robots, Wireless Body Area Network (WBAN) can be used to model communication between monitoring sensors and actuators (nodes). The communication network is used to provide critical and many ancillary information [21], [22].

WBANs are generally linked to human body applications, and is derived from Wireless Sensor Networks as a dedicated body diagnostic and monitoring network. With Soft and semi-rigid robots, WBAN can be used to monitor robot behavior and general health, with system architecture contains a central device that receives and interprets data from numerous nearby wireless sensor nodes. In WBAN applications, the devices are typically accessible, making battery replacement simple, with a long battery life expectation [23], [24].

II. RELATED WORKS

Researchers considered WBAN design and application for autonomous robots, with concentration on energy saving and ultra-low power radio aspects, using nRF52832 wireless sensor node and transmitting at 2.4 GHz [25]. Other researchers [26] considered similar energy efficiency approaches applied to wearable robots. A communication module based on human body communication was developed to wirelessly control a wearable robot hand based on myoelectric signals. The developed wireless node also transmitted at 2.4 GHz. However, the presented work in [25] and [26], did not consider structural placements of nodes with optimized nodes location.

Researchers also considered social robots that interact with the surroundings or people using sensors that are built into the robots [27]. The work presents a wearable sensor vest that is both inexpensive and open-source, together with an Internet of Things (IoT) software architecture for social humanoid robots. Sensors for touch, temperature, gesture, distance, vision, and a wireless connection module make up the vest. This work is supported by research that discusses soft and deformable robotic, wearable devices and transmitting antennas [28], [29]. The work in [27], [28], and [29], did not discuss architectural placement of nodes in terms of energy optimization.

The research in [30], [31], and [32] introduces wearable antennas that operate in the wireless body area network (WBAN), which have proliferated in a variety of industries, such as sports, rescuing, and health care. Polyester films, and ultra-thin polyimides are examples of flexible materials and techniques that have been used to maintain stable antenna radiation performance while operating in close proximity to the human body under structural bending and deformation. The work in [30], [31], and [32], did not focus on specific structural design and nodes placement and no structural placement mathematical model is presented in the work.

Communication energy and throughput analysis for skin covered robots is essential to enable optimized design of robotic WBAN. The analysis is based on modelling the robot nodes communication using WBAN principles, which is primarily used on and in human bodies as reported by researchers in [33], [34], and [35]. No physical location related coverage of body with specific design is discussed in [33], [34], and [35].

Wearable antennas are a crucial component of WBAN systems that establish a good link between in-body, on-body, and off-body devices, according to researchers in [36]. The study focuses on textile materials, which are more frequently employed as wearable antenna substrates, particularly for WBAN applications, because of their greater impedance bandwidth and reduced surface wave losses. The two primary categories of textile components are man-made and natural fibers. These materials are flexible, lightweight, easily produced, simple to incorporate into the profile of garments, and have very low dielectric constants. However, no specific nodes distribution is discussed in the work, which is critical when placement of antennas are required on robotic bodies. More researchers have also looked on wearable textile and antennas and their placements, which discussed various designs [37], [38], [39].

A thorough analysis of the wireless body area network is given in [40]. There is a detailed discussion of the WBAN communication protocols, conventional network topologies, and WBAN architectures. Also covered are the WBAN's security criteria, security concerns, different forms of attacks, and authentication methods. The study also discusses antenna designs, kinds, and flexible antennas utilized in WBAN in great depth, along with various design concerns and comparisons. The work in [40] investigates different WBAN topologies, such as mesh, star, hybrid, and tree. This leaves our work as new in terms of WBAN architecture and nodes placement. In addition, mathematical model for transition levels and transmitted packet is not presented in [40].

Researchers in [41], presented a thorough analysis of several protocols and strategies for handling, fault tolerance, and energy efficiency. The study also indicates difficulties that must be taken into account before designing and creating any WBAN architectures and protocols. The work also discussed the WBAN's architectural layout, with various sensors put on the body or on clothing that may be underneath the skin, which are also used to monitor vital indicators. Actuators are also included in the delivery of several actions. In [41], no particular WBAN nodes layout is presented.

In [41], researchers discussed clustering in relation to energy optimization. Clustering is also related to both routing and WBAN architecture. No specific architecture is presented in this work, but mainly security approach is taken towards resolving the energy and security issues. However, security is also related to nodes positioning in a WBAN network.

This work simulates data transmission using cases that represents both wearable textiles, which is similar to artificial skin, and soft robotic materials that can be used to cover robotic bodies. The work investigates energy and path loss using path loss coefficient as a factor representing the type of material in terms of channel communication and signal quality. The work uses a new design (modified X-node), which is a stable WBAN nodes distribution, and at the same time covers all parts of robotic body. This facilitates optimum and energy efficient routing.

The rest of this paper is divided as follows: Related works, Methodology, Results and Discussion, Conclusions, References.

III. METHODOLOGY

Robots that have been designed to resemble humans in some way or another are called humanoids, and they are capable of interacting with people in a natural way. Humanoids have the ability to create relationships between humans and robots that are more harmonious and natural by mimicking the looks and abilities.

In order to more closely resemble the look and feel of humans, humanoid robots' covering materials have undergone changes from rigid and heavy to soft and compliant. When considered as a whole, such new development in robotic materials demonstrates the possibility of a paradigm shift from conventional robotics to the novel concept of biologically hybrid robotics, which takes advantage of both biological and synthetic components.

As humanoids are robots that can carry out a variety of functions to interact with people in environments like healthcare, a human-like look is necessary for such duties for humanoids in order to facilitate information exchange with humans and inspire likability. The creation of humanoid covering materials with accurately simulated human skin tone and texture is essential to emulate human look.

The objective of this work is to make use of the presence of similar to human robotic skin to enable design and simulation

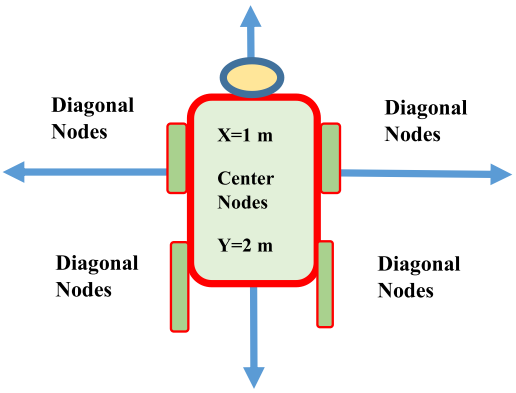

FIGURE 1. Robotic model.

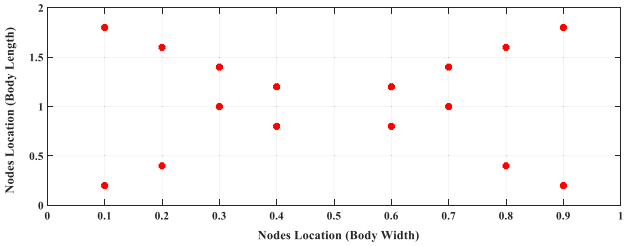

FIGURE 2. Nodes distribution over robotic body.

TABLE 1. Nomenclature.

Symbols/ Acronyms	Meaning
d	Distance between transmitter and receiver (cm)
n	Path loss exponent (between 2 and 6)
E_{Tx}	Transmission Energy (J).
E_{Rx}	Receiver energy (J).
E_{Tx} (elec)	Energy dissipated by radio transmission in the transmitter circuit (nJ/bit).
E_{Rx} (elec)	Energy dissipated by radio transmission in the receiver circuit (nJ/bit).
E_{Tx} (amp)	Energy for the transmit amplifier (nJ/bit/mn).
M	Transmitted data size.
L	Number of active nodes
E_r	Residual Energy (J)

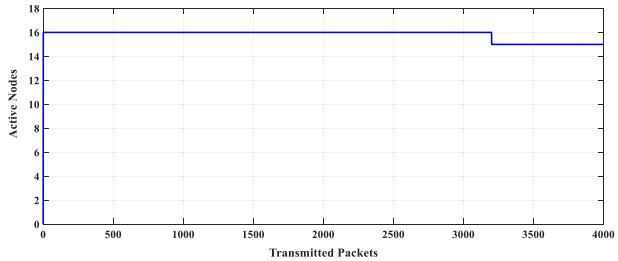

FIGURE 3. Effect of path loss coefficient on active nodes (4000 packets, n=2).

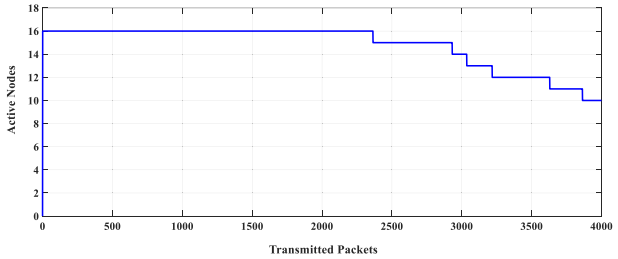

FIGURE 4. Effect of path loss coefficient on active nodes (4000 packets, n=3).

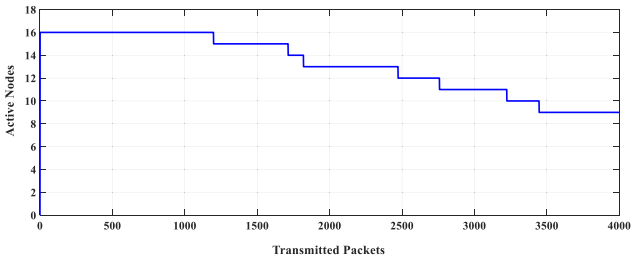

FIGURE 5. Effect of path loss coefficient on active nodes (4000 packets, n=4).

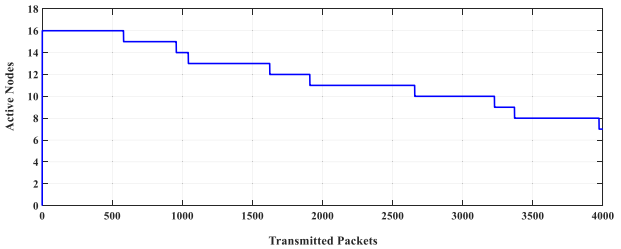

FIGURE 6. Effect of path loss coefficient on active nodes (4000 packets, n=5).

of WBANs, which are tried and tested on robots, before being used in and on humans. This approach, enables safer testing of humans, and ability to continuously enhance the efficiency of WBANs, as it is tried and tested on robots rather than humans.

The approach of this work is to analyze energy consumption in relation to message size and path loss as a function of used robotic soft materials used to build robots or to cover robots structures. The path loss coefficient represents different material types and also reflects different human skin thickness and age. Figure 1 shows the proposed robots model.

The main issue is to reach a stable WBAN design and mathematical model that can be used with soft robotics and with artificial skin covered robots. Such WBAN, will be used to try different designs on the artificial material, which has path loss similar to human skin. This way, all design and developments of WBAN networks can be carried out on robots before trying it on humans. This is important, especially that wearable antennas are used within the WBAN to enable data transmission and routing.

When considering WBAN for soft tissue robots, the following parameters should be taken into account:

1. Energy saving through the use of efficient wireless protocol and routing algorithm for data transfer to the central node.
2. Reliable radio connection to avoid missing data and transmission errors.
3. Effective communication channel: The WBAN is meant to cover only the surface area of the robot, however multiple robots may be operated simultaneously in close proximity, increasing the risk of cross-interference.
4. Flexibility through supporting of regular and irregular events.
5. Security through encryption and authentication.

In order to collect information on a variety of robotic bodily parameters, including motion and perception. Different WBAN designs are tried and tested through MATLAB simulation, with the objective of reaching a more stable design. The modified X-Node WBAN nodes structure is used in this work as a wireless network with communication between sensor nodes, with focus on less power consumption. Nodes arrangement, which are used in the simulation is shown in Figure 2. The distribution of nodes is selected to cover the whole robot body in a modified X-shape layout.

Table 1 presents definition for all used variables in the simulation and mathematical modelling.

The general form of the energy model covering soft robotic structures, is given by equations (1) and (2).

$$E_{Tx} = ME_{Tx}(elec) + nME_{Tx}(amp)\, d^n \quad (1)$$

$$E_{Rx} = ME_{Rx}(elec) \quad (2)$$

To account for different robotic materials and their propagation properties with LOS and NLOS considerations, the value of path loss exponent (n) is varied in proportion to material propagation property and antenna alignment position.

An assumption of bidirectional equal energy loss can be used to simplify calculations when taking into account energy loss owing to communication channel transmission, especially in one hop networks. It is reasonable to anticipate that some sensor nodes used for continuous monitoring will transfer data at a predetermined rate with predictable transmission intervals. This is true for robotic sensing in general, with the

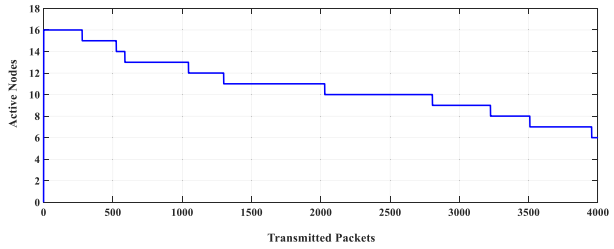

FIGURE 7. Effect of path loss coefficient on active nodes (4000 packets, n=6).

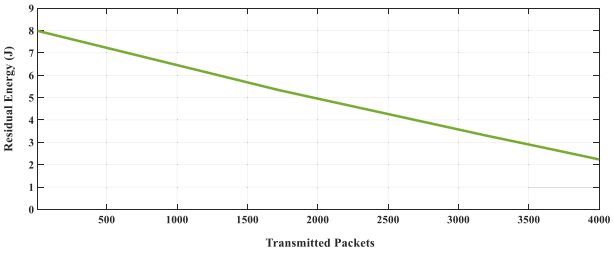

FIGURE 8. Effect of path loss coefficient on residual energy (4000 packets, n=2).

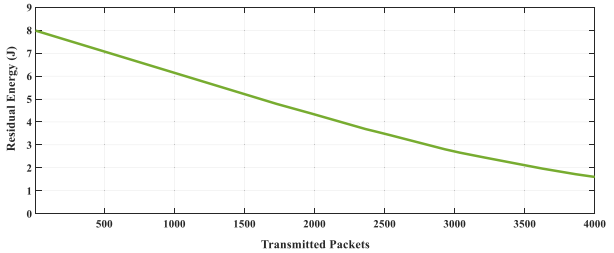

FIGURE 9. Effect of path loss coefficient on residual energy (4000 packets, n=3).

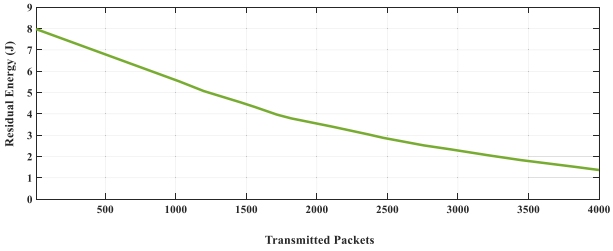

FIGURE 10. Effect of path loss coefficient on residual energy (4000 packets, n=4).

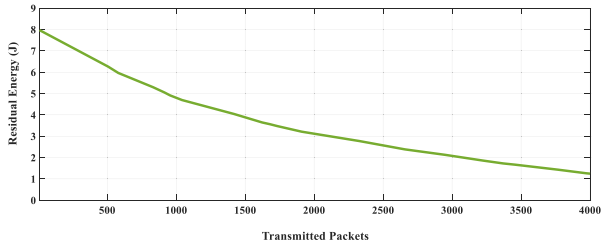

FIGURE 11. Effect of path loss coefficient on residual energy (4000 packets, n=5).

TABLE 2. Simulation parameters.

Parameter	Value
E_{Tx} (elec)	16.7 (nJ/bit).
E_{Rx} (elec)	36.1 (nJ/bit).
E_{Tx} (amp	1.97 (nJ/bit/m^n).

TABLE 3. Effect of path loss coefficient on active nodes and residual energy.

Path loss coefficient	Number of active nodes (L) at 4000 packets	Residual energy (E_r) at 4000 packets
2	15	2.4
3	10	1.6
4	9	1.4
5	7	1.2
6	6	1.1

exception of situations where an important occurrence calls for the use of event-driven transmission.

The simulation parameters used are shown in Table 2.

IV. RESULTS AND DISCUSSION

A. EFFECT OF PATH LOSS COEFFICIENT AT FIXED DATA RATE

Figures 3 to 12 present the simulation results representing effect of path loss coefficient (n) on both number of active nodes and residual energy within the nodes. The residual energy is the energy which, is taken into account to decide whether the robot nodes require recharging or can function normally. In addition, material design and build, with data rate, transmission protocol are all correlated to achieve minimum energy consumption. This will enable longer operational times for robots and more stable functionality. The detailed simulation below in Figures 3 to 12 is part of a design process to enable correlation between path loss coefficient, which is related to robot's material and nodes antenna positioning, and the required nodes energy.

The plots in Figures 3 to 7 shows the amount of data that can be transmitted per number of active nodes, before one or more of them become passive, while Figures 8-12 show the changing relationship between residual energy at maximum value of 8 Joules, which drops as a function of both transmitted data and path loss coefficient. The residual energy also changes characteristics from linear to decreasing power pattern.

From Figures 3 to 12, Table 3 is obtained, which correlates path loss coefficient to number of active nodes, and to nodes left with energy. These nodes that become passive, will be excluded from the data acquisition routes used by the channel communication protocol.

Figures 13 to 14 show the relationships between residual energy and path loss coefficient and active nodes, while

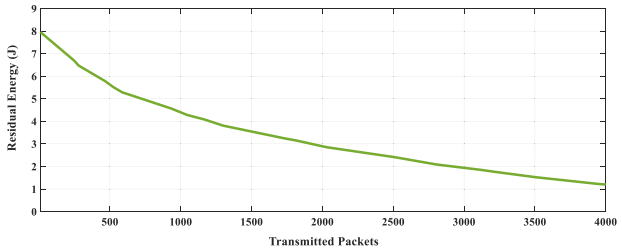

FIGURE 12. Effect of path loss coefficient on residual energy (4000 packets, n=6).

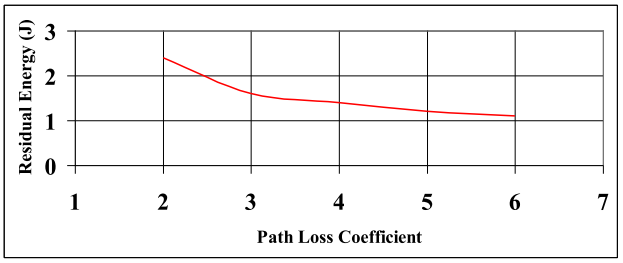

FIGURE 13. Effect of path loss coefficient on residual energy (transmitted data=4000 packets).

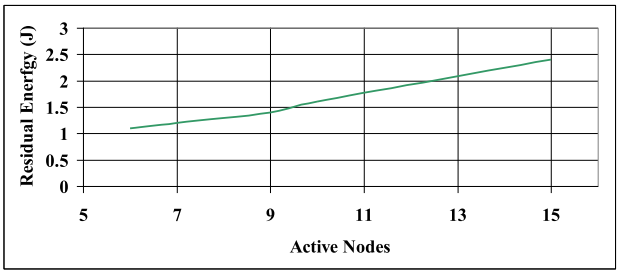

FIGURE 14. Effect of active nodes on residual energy (transmitted data=4000 packets).

Figures 15 shows the relationship between active nodes and path loss coefficient. From the plots a power relationship is apparent between the parameters as shown in equations (3) to (5).

$$E_r = \alpha n^{-k} \tag{3}$$

where;

$$\alpha \leq 4 \, and \, k \leq 0.7$$

$$E_r = \gamma L^{\rho} \tag{4}$$

where;

$$\gamma \leq 0.25 \, and \, \rho \leq 0.9$$

$$L = \beta n^{-\mu} \tag{5}$$

where;

$$\beta \leq 26 \, and \, \mu \leq 0.8$$

Table 4 represents a relationship between the numbers of active nodes left after transmitting certain number of packets as a function of path loss coefficient. This is an important

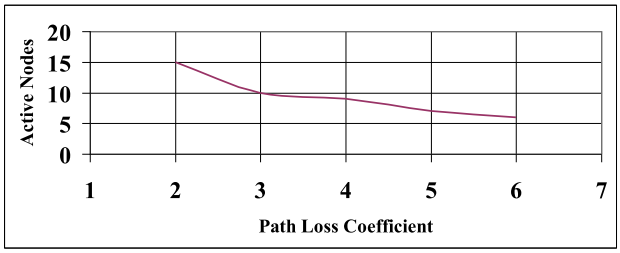

FIGURE 15. Effect of path loss coefficient on remaining active nodes (transmitted data=4000 packets).

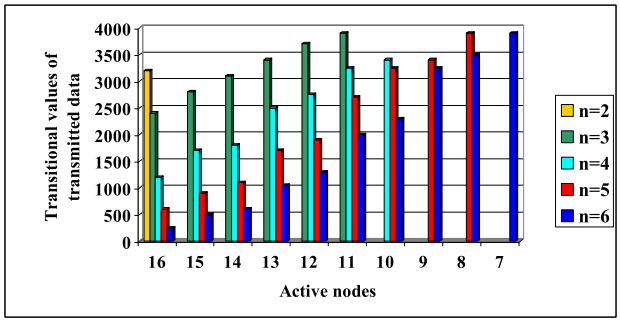

FIGURE 16. Effect of path loss coefficient on transmitted data pattern (transmitted data=4000 packets).

TABLE 4. Transition levels of active nodes to passive nodes as a function of path loss exponent and fixed data rate.

Node Transition	Path loss coefficient (n)				
	2	3	4	5	6
	Transmitted packets : Transition values				
16➔15	3200	2400	1200	600	250
15➔14	-	2800	1700	900	500
14➔13	-	3100	1800	1100	600
13➔12	-	3400	2500	1700	1050
12➔11	-	3700	2750	1900	1300
11➔10	-	3900	3250	2700	2000
10➔9	-	-	3400	3250	2300
9➔8	-	-	-	3400	3250
8➔7	-	-	-	3900	3500
7➔6	-	-	-	-	3900

Table for robotic material design and choice of number of nodes to enable transmission of desired amount of data.

Table 4 shows that for example, to transmit 4000 packets at path loss coefficient of n=2, then 3200 are transmitted with 16 active nodes, and the rest (800 packets) are transmitted with 15 active nodes, as one node will lose energy and becomes passive. This means that to complete the 4000 packets transmission, at n=2, the 16 active nodes become 15 active nodes. Another example, is to transmit 4000 packets at path loss coefficient, n=4, only 1200 packets are transmitted with all 16 nodes active, with the rest of packets (2800 packets)

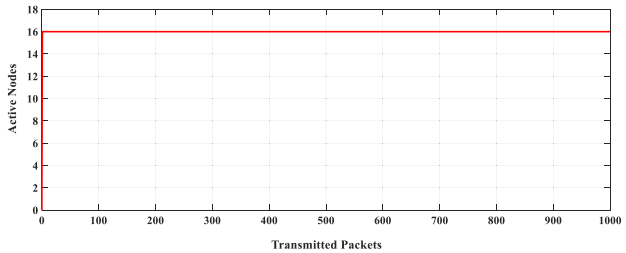

FIGURE 17. Effect of data size at fixed path loss coefficient on active nodes (1000 packets, n=6).

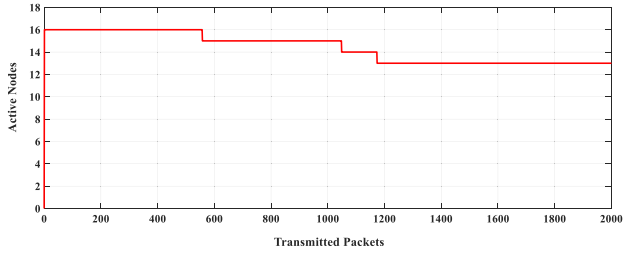

FIGURE 18. Effect of data size at fixed path loss coefficient on active nodes (2000 packets, n=6).

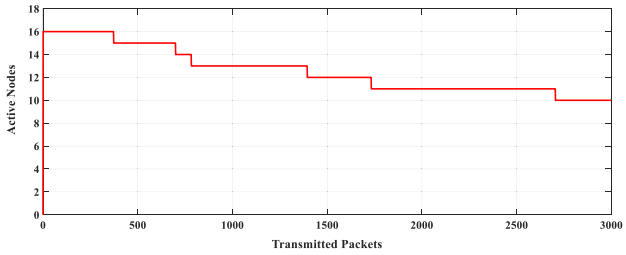

FIGURE 19. Effect of data size at fixed path loss coefficient on active nodes (3000 packets, n=6).

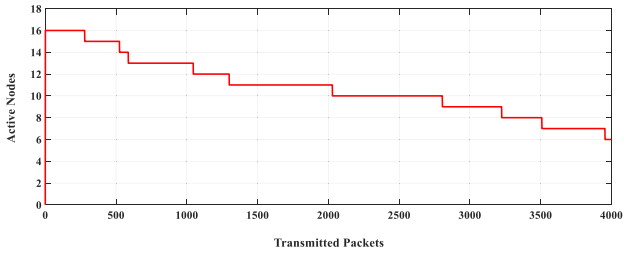

FIGURE 20. Effect of data size at fixed path loss coefficient on active nodes (4000 packets, n=6).

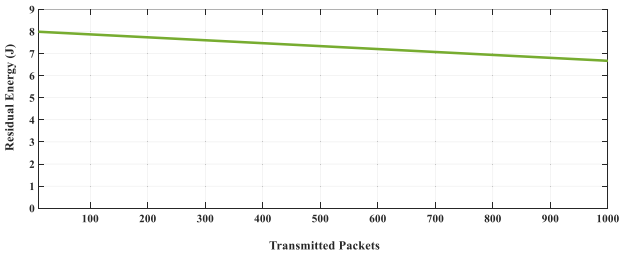

FIGURE 21. Effect of data size at fixed path loss coefficient on residual energy (1000 packets, n=6).

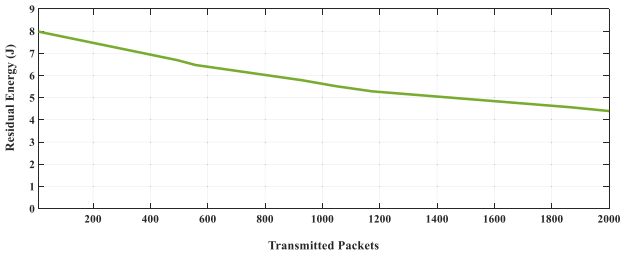

FIGURE 22. Effect of data size at fixed path loss coefficient on residual energy (2000 packets, n=6).

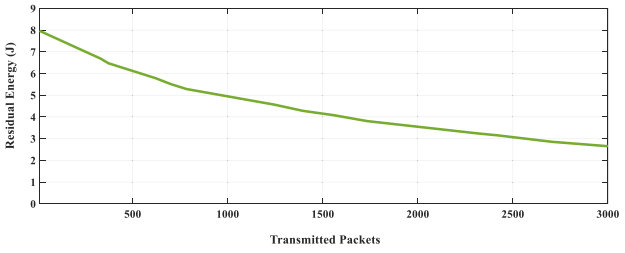

FIGURE 23. Effect of data size at fixed path loss coefficient on residual energy (3000 packets, n=6).

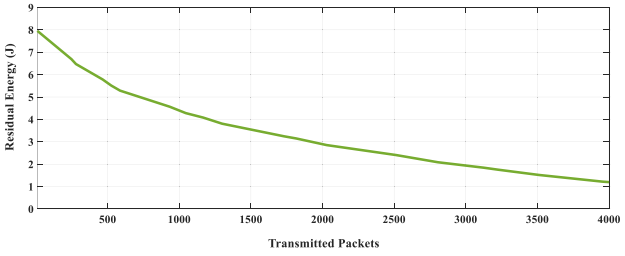

FIGURE 24. Effect of data size at fixed path loss coefficient on residual energy (4000 packets, n=6).

are transmitted over routes chosen to bypass passive nodes, leaving only 7 active nodes at 4000 packets.

Table 4 clearly shows the effect of path loss coefficient on ability to transmit data effectively. This coefficient is directly related to the type of material used to cover robotic body and also to selected routes. The table, also shows that as the pat loss coefficient is reduced, less nodes are required to enable same message size transmission, which will also help in shortening the required routes to destination or sink.

Figure 16 shows a comparison of different path loss coefficients and their effect on transitional data transmitted and number of active nodes. The pattern allows for design modification of robotic structures and nodes placement.

B. EFFECT OF DATA SIZE AT FIXED PATH LOSS COEFFICIENT

Figures 17 to 24 present the simulation results representing effect of transmitted data, for fixed path loss coefficient

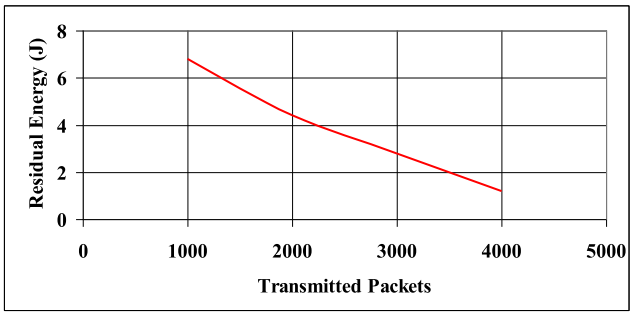

FIGURE 25. Effect of data size on residual energy (n=6).

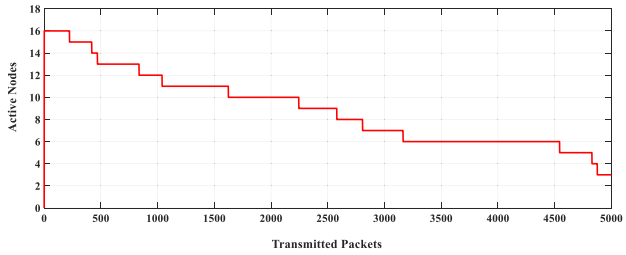

FIGURE 26. Effect of data size at fixed path loss coefficient on active nodes (5000 packets, n=6).

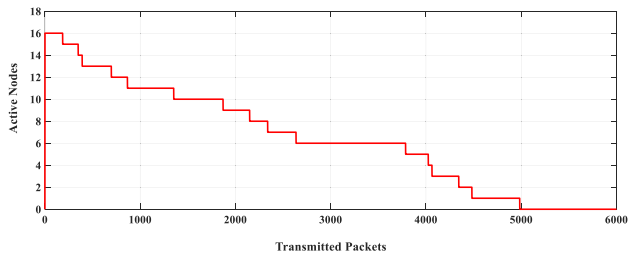

FIGURE 27. Effect of data size at fixed path loss coefficient on active nodes (6000 packets, n=6).

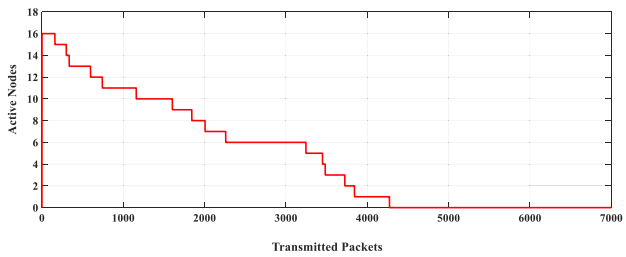

FIGURE 28. Effect of data size at fixed path loss coefficient on active nodes (7000 packets, n=6).

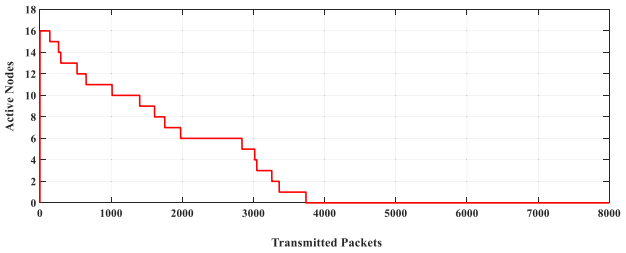

FIGURE 29. Effect of data size at fixed path loss coefficient on active nodes (8000 packets, n=6).

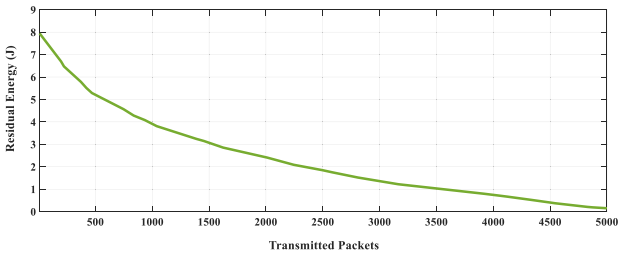

FIGURE 30. Effect of data size at fixed path loss coefficient on residual energy (5000 packets, n=6).

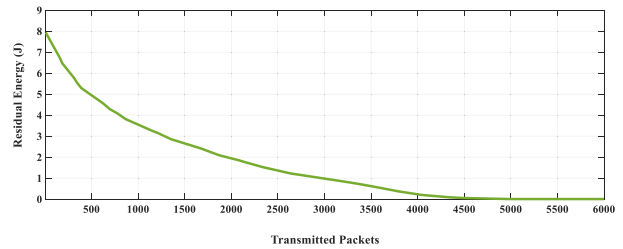

FIGURE 31. Effect of data size at fixed path loss coefficient on residual energy (6000 packets, n=6).

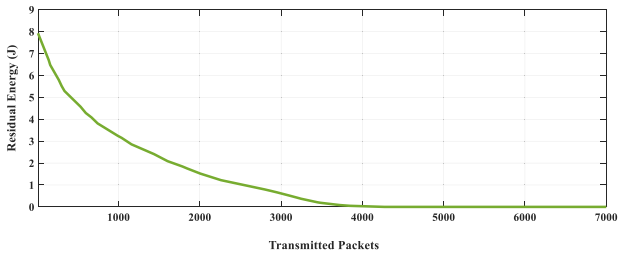

FIGURE 32. Effect of data size at fixed path loss coefficient on residual energy (7000 packets, n=6).

(n=6), on both, number of active nodes and residual energy within the specified device transmission data size.

From the plots, it is evident that the larger the data size, more energy is consumed due to the increment in transmitted data. At realized from Figures 21 to 24, the behavior of the nodes starts from linear, and then as data transmission increases, it followed non-linear path similar to an exponential, which is consistent with energy reduction process and routing process. The relationship between residual energy and data size is presented in Figure 25, with its mathematical expression presented in equation (6).

$$E_r = \theta exp\,(-\phi M) \tag{6}$$

where;

$$\theta \geq 13 \; and \; \phi \leq 0.001$$

Using equations (4) and (6), equation (7) is obtained.

$$\gamma L^{\rho} = \theta exp\,(-\phi M) \tag{7}$$

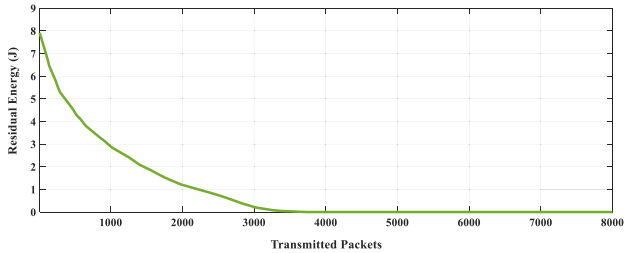

FIGURE 33. Effect of data size at fixed path loss coefficient on residual energy (8000 packets, n=6).

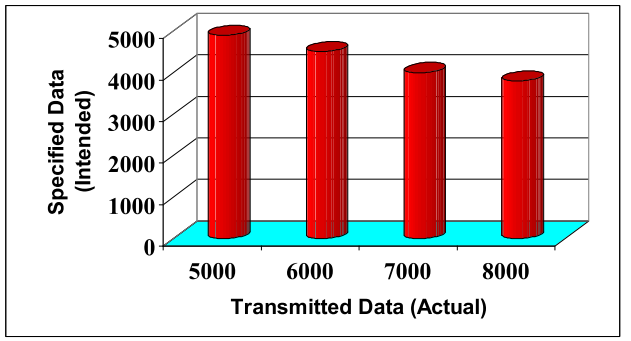

FIGURE 34. Relationship between device specified data and transmitted data (n=6).

From equation (7), equation (8) is obtained.

$$L^{\rho} = \left(\frac{\theta exp\,(-\phi M)}{\gamma}\right) \tag{8}$$

From equation (8), an important expression is obtained relating number of active nodes (L) to data size (M), as in equation (9).

$$L = \left(\frac{\theta exp\,(-\phi M)}{\gamma}\right)^{1/\rho} \tag{9}$$

The parameters in equation (9) can be used during the design process to enable data size optimization related to number of used nodes and number of still active nodes.

C. EFFECT OF TRANSMITTING ABOVE THE SPECIFIED DATA SIZE

Figures 26 to 32 show effect of transmitting above nodes rated data size with a large number of nodes (L=16) in this case. From the plots, it is clear that the energy of the nodes rapidly consumed and depleted as larger data is transmitted before a re-charge occurs to the participating nodes. (M $>$ 4000 packets). Thus, different recharging mechanism is required, and shorter routes should be considered. In addition, lower path loss coefficient, should always be considered to preserve energy.

Figures 30 to 33, also show that as intended data size increases, the actual data transmitted is reduced as the residual energy is dramatically affected. For example, if the intended data size to be transmitted is 6000 packets, the actual transmitted data is 4500 packets, after that total energy depletion occurs. Another example, if the intended data to be transmitted is 7000 packets, the actual transmitted data is 4000 packets, after which, no data can be transmitted.

Figure 34 show the relationship between intended data size and transmitted data. The relationship with an average reduction coefficient of 0.7 is described by equation (10).

$$M_{transmitted} = \kappa M_{intended} \tag{10}$$

where;

$$0.5 \leq \kappa \leq 1$$

Using equation (9) and applying equation (10), results in equation (11), which describes the actual active nodes and can be used in the design stage.

$$L_{actual} = \left(\frac{\theta exp\,(-\phi \kappa M_{intended})}{\gamma}\right)^{1/\rho} \tag{11}$$

V. CONCLUSION

The work found through simulation and mathematical modeling of Modified X-shape node distribution on robotic structures, that human wearable sensor approach can be applied to soft robots, and robotic structures covered with artificial skin. This is possible due to similar path loss coefficients for synthetic materials to human body, with similar path loss coefficients.

The presented research work, established an inverse relationship between residual energy and path loss coefficient, and similar one between residual energy and data size. Also, a mathematical model is presented relating desired data to be transmitted to the actual data that can be transmitted before total depletion of energy occurs. Such depletion is also related to routing, number of nodes, and device specifications.

The work provides an initial mathematical model to enable design of WBANs that are tested on robotic structures with artificial skin and soft robotics, before using such nodes and networks on humans. This is important as they include wearable antennas

ACKNOWLEDGMENT

A modified version of simulation software is used, which is initially prepared by Qaisar Nadeem of the COMSENSE research group.

REFERENCES

[1] N. Gariya and P. Kumar, "A review on soft materials utilized for the manufacturing of soft robots," *Mater. Today, Proc.*, vol. 46, pp. 11177–11181, Jan. 2021.
[2] C. Armanini, F. Boyer, A. T. Mathew, C. Duriez, and F. Renda, "Soft robots modeling: A structured overview," *IEEE Trans. Robot.*, vol. 39, no. 3, pp. 1728–1748, Jun. 2023.
[3] O. Yasa, Y. Toshimitsu, M. Y. Michelis, L. S. Jones, M. Filippi, T. Buchner, and R. K. Katzschmann, "An overview of soft robotics," *Annu. Rev. Control, Robot., Auto. Syst.*, vol. 6, pp. 1–29, May 2023.
[4] F. Schmitt, O. Piccin, L. Barbé, and B. Bayle, "Soft robots manufacturing: A review," *Frontiers Robot. AI*, vol. 5, pp. 2–17, Jul. 2018.
[5] L. Chen, C. Yang, H. Wang, D. T. Branson, J. S. Dai, and R. Kang, "Design and modeling of a soft robotic surface with hyperelastic material," *Mechanism Mach. Theory*, vol. 130, pp. 109–122, Dec. 2018.

[6] A. López-González, J. Tejada, and J. López-Romero, "Review and proposal for a classification system of soft robots inspired by animal morphology," *Biomimetics*, vol. 8, no. 2, pp. 1–28, 2023.
[7] F. Stella and J. Hughes, "The science of soft robot design: A review of motivations, methods and enabling technologies," *Frontiers Robot. AI*, vol. 9, pp. 1–8, Jan. 2023.
[8] M. P. Venter and I. Joubert, "Generative design of soft robot actuators using ESP," *Math. Comput. Appl.*, vol. 28, no. 2, pp. 1–17, 2023.
[9] M. Dubied, M. Y. Michelis, A. Spielberg, and R. K. Katzschmann, "Sim-to-real for soft robots using differentiable FEM: Recipes for meshing, damping, and actuation," *IEEE Robot. Autom. Lett.*, vol. 7, no. 2, pp. 5015–5022, Apr. 2022.
[10] J. Wang and A. Chortos, "Control strategies for soft robot systems," *Adv. Intell. Syst.*, vol. 4, no. 5, pp. 1–27, May 2022.
[11] M. Grube, J. Wieck, and R. Seifried, "Comparison of modern control methods for soft robots," *Sensors*, vol. 22, no. 23, pp. 1–24, 2022.
[12] H. Yang and W. Wu, "A review: Machine learning for strain sensor-integrated soft robots," *Frontiers Electron. Mater.*, vol. 2, pp. 1–8, Nov. 2022.
[13] J. Shu, J. Wang, S. Lau, Y. Su, K. Heung, X. Shi, Z. Li, and R. K.-Y. Tong, "Soft robots' dynamic posture perception using kirigami-inspired flexible sensors with porous structures and long short-term memory (LSTM) neural networks," *Sensors*, vol. 22, no. 20, pp. 1–18, 2022.
[14] N. El-Atab, R. B. Mishra, F. Al-Modaf, L. Joharji, A. A. Alsharif, H. Alamoudi, M. Diaz, N. Qaiser, and M. M. Hussain, "Soft actuators for soft robotic applications: A review," *Adv. Intell. Syst.*, vol. 2, no. 10, pp. 1–37, Oct. 2020.
[15] B. Oh, Y.-G. Park, H. Jung, S. Ji, W. Cheong, J. Cheon, W. Lee, and J.-U. Park, "Untethered soft robotics with fully integrated wireless sensing and actuating systems for somatosensory and respiratory functions," *Soft Robot.*, vol. 7, no. 5, pp. 564–573, 2020.
[16] O. Gul, "Energy harvesting and task-aware multi-robot task allocation in robotic wireless sensor networks," *Sensors*, vol. 23, no. 6, pp. 1–19, 2023.
[17] H. Huang, A. V. Savkin, M. Ding, and C. Huang, "Mobile robots in wireless sensor networks: A survey on tasks," *Comput. Netw.*, vol. 148, pp. 1–19, Jan. 2019.
[18] J. H. Ryu, M. Irfan, and A. Reyaz, "A review on sensor network issues and robotics," *J. Sensors*, vol. 2015, pp. 1–14, Aug. 2015.
[19] D. M. G. Preethichandra, L. Piyathilaka, U. Izhar, R. Samarasinghe, and L. C. De Silva, "Wireless body area networks and their applications—A review," *IEEE Access*, vol. 4, pp. 1–20, 2016.
[20] G. Rajesh, X. M. Raajini, N. Kritika, A. Kavinkumar, K. M. Sagayam, M. H. A. Wahab, and M. M. Som, "Achieving longevity in wireless body area network by efficient transmission power control for IoMT applications," *Int. J. Integr. Eng.*, vol. 14, no. 3, pp. 80–89, Jun. 2022.
[21] R. Li, D. T. H. Lai, and W. Lee, "A survey on biofeedback and actuation in wireless body area networks (WBANs)," *IEEE Rev. Biomed. Eng.*, vol. 10, pp. 162–173, 2017.
[22] Y. Wang, R. Liu, M. Shu, and C. Chen, "Stochastic geometry analysis of throughput for wireless body area networks," *Adv. Robot. Autom.*, vol. 6, no. 3, pp. 1–6, 2017.
[23] A. Dawod, B. Hakim, A. Radhi, Z. Jabbar, J. Tawfeq, and P. S. JosephNg, "A novel nomadic people optimizer-based energy-efficient routing for WBAN," *Periodicals Eng. Natural Sci.*, vol. 11, no. 3, pp. 97–108, 2023.
[24] M. Munih, Z. Ivanić, and R. Kamnik, "Wearable sensory apparatus for real-time feedback in wearable robotics," *Appl. Sci.*, vol. 11, no. 23, pp. 1–21, 2021.
[25] L. Gisin, H. D. Doran, and J.-M. Gruber, "RoboBAN: A wireless body area network for autonomous robots," in *Proc. 13th Int. Conf. Informat. Control, Autom. Robot.*, vol. 2, 2016, pp. 49–60.
[26] T. Iguchi, I. Kondo, and J. Wang, "Wireless control combining myoelectric signal and human body communication for wearable robots," *Micromachines*, vol. 13, no. 12, pp. 1–12, 2022.
[27] M. Jafarzadeh, S. Brooks, S. Yu, B. Prabhakaran, and Y. Tadesse, "A wearable sensor vest for social humanoid robots with GPGPU, IoT, and modular software architecture," *Robot. Auto. Syst.*, vol. 139, pp. 1–31, May 2021.
[28] Y. B. Chaouche, M. Nedil, M. Olaimat, M. E. Badawe, and O. M. Ramahi, "Wearable metasurface antenna based on electrically-small ring resonators for WBAN applications," *Electron. Lett.*, vol. 58, no. 1, pp. 4–7, 2022.
[29] I. Aitbar, N. Shoaib, A. Alomainy, A. Quddious, S. Nikolaou, M. Ali Imran, and Q. H. Abbasi, "AMC integrated multilayer wearable antenna for multiband WBAN applications," *Comput., Mater. Continua*, vol. 71, no. 2, pp. 3227–3241, 2022.
[30] Q. Liu, K. G. Mkongwa, and C. Zhang, "Performance issues in wireless body area networks for the healthcare application: A survey and future prospects," *SN Appl. Sci.*, vol. 3, pp. 1–19, Jan. 2021.
[31] M. Yaghoubi, K. Ahmed, and Y. Miao, "Wireless body area network (WBAN): A survey on architecture, technologies, energy consumption, and security challenges," *J. Sensor Actuator Netw.*, vol. 11, no. 4, pp. 1–34, 2022.
[32] R. Goyal, N. Mittal, L. Gupta, and A. Surana, "Routing protocols in wireless body area networks: Architecture, challenges, and classification," *Wireless Commun. Mobile Comput.*, vol. 2023, pp. 1–19, Jan. 2023.
[33] J. Boga and V. D. Kumar, "Human activity recognition by wireless body area networks through multi-objective feature selection with deep learning," *Expert Syst.*, vol. 39, no. 8, pp. 1–12, Sep. 2022.
[34] S. B. U. D. Tahir, A. Jalal, and K. Kim, "Wearable inertial sensors for daily activity analysis based on Adam optimization and the maximum entropy Markov model," *Entropy*, vol. 22, no. 5, pp. 1–19, 2020.
[35] A. Hamdi, A. Nahali, M. Harrabi, and R. Brahem, "Optimized design and performance analysis of wearable antenna sensors for wireless body area network applications," *J. Inf. Telecommun.*, vol. 7, no. 2, pp. 155–175, Apr. 2023.
[36] H. Muhammad, Y. I. Abdulkarim, P. A. Abdoul, and J. Dong, "Textile and metasurface integrated wide-band wearable antenna for wireless body area network applications," *AEU, Int. J. Electron. Commun.*, vol. 169, pp. 1–6, Sep. 2023.
[37] P. B. Samal, S. J. Chen, and C. Fumeaux, "Wearable textile multiband antenna for WBAN applications," *IEEE Trans. Antennas Propag.*, vol. 71, no. 2, pp. 1391–1402, Feb. 2023.
[38] S. Hussain, S. Hafeez, S. Ali, and N. Pirzada, "Design of wearable patch antenna for wireless body area networks," *Int. J. Adv. Comput. Sci. Appl.*, vol. 9, no. 9, pp. 147–151, 2018.
[39] M. M. H. Mahfuz, M. R. Islam, C.-W. Park, E. A. A. Elsheikh, F. M. Suliman, M. H. Habaebi, N. A. Malek, and N. Sakib, "Wearable textile patch antenna: Challenges and future directions," *IEEE Access*, vol. 10, pp. 38406–38427, 2022.
[40] D. M. G. Preethichandra, L. Piyathilaka, U. Izhar, R. Samarasinghe, and L. C. De Silva, "Wireless body area networks and their applications—A review," *IEEE Access*, vol. 11, pp. 9202–9220, 2023.
[41] S. Singh and D. Prasad, "Wireless body area network (WBAN): A review of schemes and protocols," *Mater. Today, Proc.*, vol. 49, pp. 3488–3496, Jan. 2022.

MAHMOUD Z. ISKANDARANI (Member, IEEE) received the B.Eng. degree (Hons.) in engineering electronics and the M.Sc. degree in engineering electronics (analogue neural processor) from the University of Warwick, U.K., in 1990 and 1992, respectively. After that he carried out research with the Advanced Technology Center, University of Warwick, in smart classification techniques used in non-destructive testing of composite structures, employing thermal imaging, ultrasonic sensors, and other sensing devices together with neural networks leading him to receiving the Ph.D. degree in engineering, in 1996. He is currently a Full Professor with Al-Ahliyya Amman University, Amman, Jordan, lecturing postgraduates in intelligent transportation systems with the Faculty of Engineering, and carrying out research in sensors, VANETs communication, and intelligent algorithms applied to transportation and robotic structures. He leads two research groups with the Faculty of Engineering: the Engineering Research Group for Intelligent Transportation Systems (EITSRG) and the Electronic Sensors Research Group (ESRG). He has authored over 90 peer refereed papers. His research interests include sensors and their application in E-nose, wireless sensor networks, wireless body area networks, and intelligent transportation systems with particular interest in neural networks. He is a member of ITSS and VTS.